

Electronic properties of Fe clusters on a Au(111) surface

Alexandre Delga,¹ Jérôme Lagoute,¹ Vincent Repain,¹ Cyril Chacon,¹ Yann Girard,¹ Madhura Marathe,² Shobhana Narasimhan,² and Sylvie Rousset¹

¹Laboratoire Matériaux et Phénomènes Quantiques, Université Paris diderot-Paris 7, UMR CNRS 7162, 10 rue Alice Domon et Léonie Duquet, F-75205 Paris Cedex 13, France

²Theoretical Sciences Unit, Jawaharlal Nehru Centre for Advanced Scientific Research, Jakkur, Bangalore 560064, India

(Received 11 March 2011; published 21 July 2011)

The electronic states of self-organized Fe nanoislands on a Au(111) surface have been investigated using low-temperature scanning tunneling microscopy and spectroscopy. We show that the local density of states is dominated by Shockley surface states confined in the nanostructures. Comparing the experimental dispersion diagram with a free-electron model we derive the effective mass $m^* = 0.39 m_e$ and the band onset $E_0 = -420$ meV of these states. *Ab initio* calculations show the existence of the Shockley surface states in the Fe layer, in agreement with the experiment, and reveal that they are fully spin polarized.

DOI: [10.1103/PhysRevB.84.035416](https://doi.org/10.1103/PhysRevB.84.035416)

PACS number(s): 68.37.Ef, 73.20.-r, 73.22.-f

I. INTRODUCTION

The physics of low-dimensional systems has attracted wide interest in recent years because of the fascinating new physical properties arising with the size reduction of materials. In particular, nanostructures grown at the surface of metallic substrates are a rich playground for the investigation of new magnetic, electronic, or catalytic properties. The constant demand for increased data storage density and the recent development of spin electronics has motivated a number of research efforts in magnetic systems with reduced dimensions. In this context, magnetic nanoislands grown on nanopatterned surfaces are promising model systems due to their ability to produce arrays of magnetic nanostructures self-organized over a very large scale. The Au(111) surface is particularly interesting because its so-called herringbone reconstruction provides a natural template on which as-grown metallic material can lead to the formation of self-organized nanostructures. Self-organization has been demonstrated on that substrate with several materials such as Fe,¹⁻³ Co,⁴ Ni,⁵ and Cr.⁶ The case of Fe/Au(111) is particularly interesting since its magnetism depends on its atomic structure which changes drastically with the amount of deposition from nanoislands to one-dimensional (1D) nanowires and finally a two-dimensional (2D) film. X-ray magnetic circular dichroism studies have demonstrated that during the growth process unexpected magnetic behavior occurs with an in-plane anisotropy observed in nanoislands.⁷ For a complete understanding of the physics of the Fe/Au(111) system it is necessary to get detailed knowledge of its electronic structure. The electronic properties of Fe nanostructures on a gold substrate have been investigated using angle-resolved photoemission spectroscopy on Fe wires grown at the step edges of a vicinal Au substrate.⁸ However there are currently no data available on the electronic properties of Fe nanostructures on Au(111). Scanning tunneling microscopy (STM) and spectroscopy (STS) are techniques particularly adapted to the investigation of the local electronic structure of nanometer-size objects because they allow one to combine lateral atomic resolution with local spectroscopy. Here we intend to shed more light on the electronic properties of Fe nanostructures on Au(111) by performing STM/STS measurements. We provide experimental evidence of a Shock-

ley surface state at the surface of the Fe islands. Local spectra show a series of peaks which are attributed to confined states. Conductance images provide a visualization of the corresponding spatial distribution of the electron density. Comparing the experimental data with a free-electron model we show that the observed wave patterns correspond to confined states in the islands. The comparison of calculated and experimental energies of those states allows us to estimate the effective mass $m^* = 0.39 m_e$ and the band onset $E_0 = -420$ meV. *Ab initio* calculations reveal the existence of two surface states on the Fe layer, one that has a *d*-like character and is not accessible to the STM tip due to a small extension in the vacuum, and the other that is the Shockley surface state. In good agreement with experiment, the latter is found to have a band onset shifted to higher energy and a larger effective mass compared to the bare Au(111) surface while the *d*-like state has a band onset shifted to lower energy as compared to clean Au(111). As a consequence the dispersive state measured in the experiment can be identified as the Shockley surface state. The calculations also reveal that the Shockley surface state in Fe is fully spin polarized. The spin polarization of such states has been previously evidenced experimentally and theoretically on the Co/Cu(111) system.⁹⁻¹¹ We then compare the free-electron model with a tight-binding description of the Fe islands that can also reproduce the experimental data. The latter approach allows us to discuss edge effects on nanoislands measured by STM. In particular the appearance of bright edges in topography and their influence in the conductance maps are discussed and can be attributed to confined Shockley surface states without a specific edge state.

II. EXPERIMENTAL SETUP

Experiments have been performed with an Omicron Nanotechnology LT-STM. The STM chamber (tip and sample) was cooled by liquid He down to 5 K, and under ultrahigh vacuum ($P \approx 10^{-10}$ mbar). The Au(111) sample was cleaned by repeated cycles of Ar⁺ sputtering and 750 K annealing. Iron was evaporated at room temperature under ultrahigh vacuum by sublimation of a Fe rod. The measurements were performed

at 5 K with an electrochemically etched tungsten tip. Local dI/dV spectra were obtained with the *lock-in* technique. The conductance maps were recorded in the current imaging tunneling spectroscopy (CITS) mode. Spectra were taken at every pixel of the topographic image, consequently enabling one to recreate conductivity dI/dV maps of the local density of states (LDOS) at a given energy. One has to note that in these methods the sample LDOS is measured along the tip trajectory.

III. RESULTS AND DISCUSSION

Figure 1 shows the surface after a deposition of 0.13 ML of Fe on Au(111) at room temperature. The kinks of the Au(111) reconstruction act as nucleation centers that, upon Fe deposition, lead to the formation of self-organized Fe clusters with a monolayer height for a coverage below 0.3 ML.¹ Above this coverage, the clusters coalesce along the $\langle 11\bar{2} \rangle$ direction and nanowires appear. The atomic structure of self-organized clusters has been studied and it was shown that they grow in a pseudomorphic way.^{2,12} The shapes of the clusters are polygonal, most of them being triangles or truncated triangles. Their orientation follows that of the underlying reconstruction.

We investigated the local electronic structure of the Fe clusters by performing STS on several islands. A typical example is presented in Fig. 2. The dI/dV spectrum displayed in Fig. 2(a) was measured close to the center of the island shown in the inset. Four peaks clearly appear at -0.10 , 0.08 , 0.45 , and 1.20 eV. The respective intensity of these peaks strongly depends on the location where the spectrum is measured, indicating that the corresponding electronic states have strong spatial inhomogeneity. In order to identify the origin of these peaks we measured dI/dV maps at

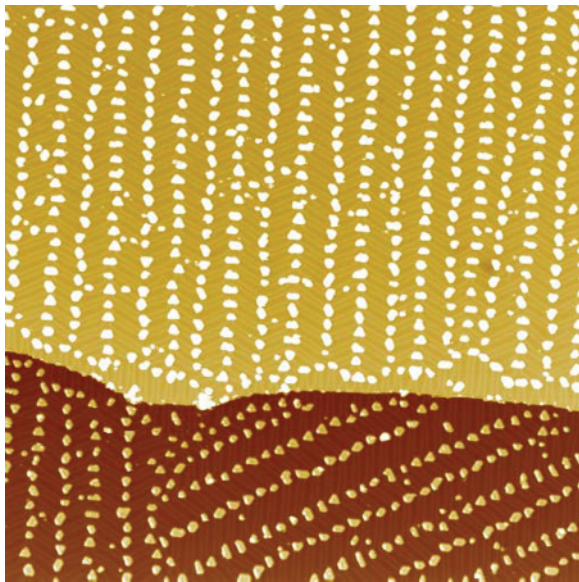


FIG. 1. (Color online) Fe/Au(111) topographic 300×300 nm² STM image measured at 5 K, with a 1 V bias and a 0.13 ML coverage of Fe deposited at room temperature. Two out of the three different herringbone reconstruction directions can be seen, as well as their impact on the clusters' orientation.

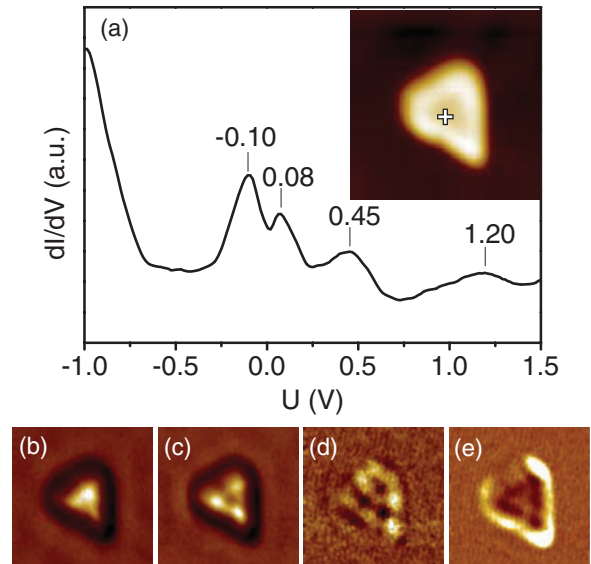


FIG. 2. (Color online) (a) dI/dV spectrum measured close to the center of a Fe/Au(111) cluster. The inset shows a 10×10 nm² STM image of the Fe cluster measured at a bias of 1 V; the cross indicates the location where the spectrum was measured. (b)–(e) dI/dV maps measured in the CITS mode at energies corresponding to the peaks in the spectroscopy, respectively -0.09 , 0.07 , 0.55 , and 1.18 eV.

energies corresponding to these states. The resulting images are displayed in Figs. 2(b)–2(e). The best contrast in the images is not always found exactly at the energy of the peak determined in the spectrum, and as a consequence the images displayed are obtained at energies slightly different from those shown in the spectrum. While the first state at -0.10 eV is almost featureless with an electron density concentrated at the center, the next three states exhibit one, three, and six nodes, respectively. These features are close to that of the first four states of a free electron wave confined in a triangular box (see more details below). These results indicate that Shockley-like surface states are present at the surface of the Fe nanoclusters. In order to confirm this interpretation we performed STS on several islands with similar shapes but different sizes. In Fig. 3 we plot the measured energy position of the peaks as a function of the size of the clusters. Clearly the position of the peaks depends on the cluster size and shifts to lower energy when the area increases as expected for confined states. We compared this experimental dispersion diagram with the one given by a free-electron model.

A. Spectral analysis

We used a particle-in-a-box model with Dirichlet boundary conditions.¹³ We verified that the computational method we used gives the same energies as the analytical solutions in a pure triangle. The main asset of this model is that any convex geometry is computable. We have chosen a truncated triangular shape¹⁴ of surface area S with a long to short edge ratio of 2.73 which is very close to the mean experimental shape of clusters studied in Fig. 3.

This model gives a set of eigenenergies $E_n = E_0 + \frac{\lambda_n}{m^*S}$ where E_n are the energies for different modes, E_0 is the band

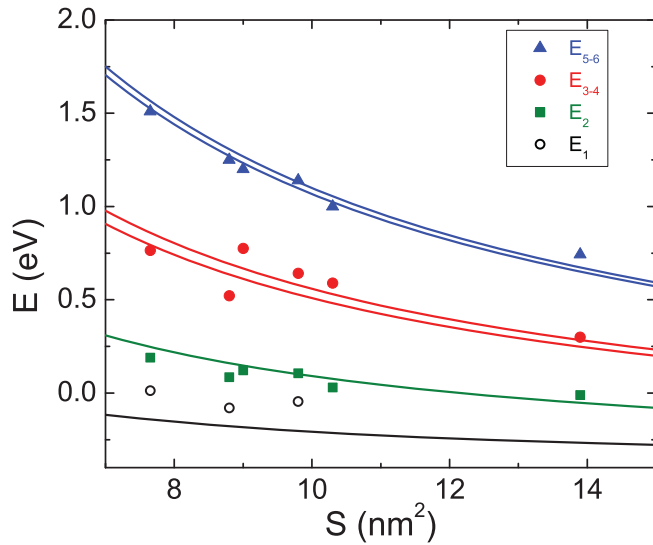


FIG. 3. (Color online) Energy positions of the spectroscopy peaks as a function of the surface area of the Fe clusters. Markers indicate experimental data measured on different islands with truncated triangular shape. Black open circles correspond to the lower energy state. Green squares, red closed circles, and blue triangles correspond to the first, second, and third excited states, respectively. The lines correspond to the calculated energies of the first six states (from bottom to top) of free-electron confined states in a truncated triangular box.

onset of the 2D electron gas, and m^* is the effective mass. λ_n are calculated eigenvalues in atomic units: $\lambda_1 = 10.87$, $\lambda_2 = 26.14$, $\lambda_3 = 47.56$, $\lambda_4 = 50.11$, $\lambda_5 = 76.17$, and $\lambda_6 = 77.80$, where the second, fourth, and sixth states are doubly degenerate.

The values of λ_3 and λ_4 are very close (as can be seen in Fig. 3 they lead to two dispersion curves very close together). Due to the energy broadening, it is expected that the corresponding states could not be resolved in the experiment and should appear in the experimental spectrum as one single peak. The same observation can be done for λ_5 and λ_6 . Therefore, we used the respective mean value of these two pairs of states to compare with the experimental energies that we denoted E_{3-4} and E_{5-6} . To find the effective mass and band onset, we have fitted the experimental data with the calculated eigenenergies, and we have chosen not to take into account the state at E_1 . Indeed, it is actually very difficult to single out the ground state of the confined Shockley surface state for two reasons: first, it is almost featureless in the spatial mapping (maximum at the center) and therefore difficult to identify in the dI/dV maps [see Fig. 2(b)]. Second, it is almost dispersionless in our experimental size range and can therefore be mixed up with a d -band state. Using this procedure, we find $m^*/m_e = 0.39 \pm 0.1$, where m_e is the electronic mass, and $E_0 = -420 \pm 50$ meV. These values are close to the Shockley surface state of Au(111) (where $m^*/m_e = 0.26 \pm 0.01$ and $E_0 = -520 \pm 10$ meV¹⁵), but they indicate that on the Fe island the band onset is shifted by 100 meV above the onset of the bare Au(111) surface and the effective mass is larger. In Fig. 3, a discrepancy can be observed between the calculated

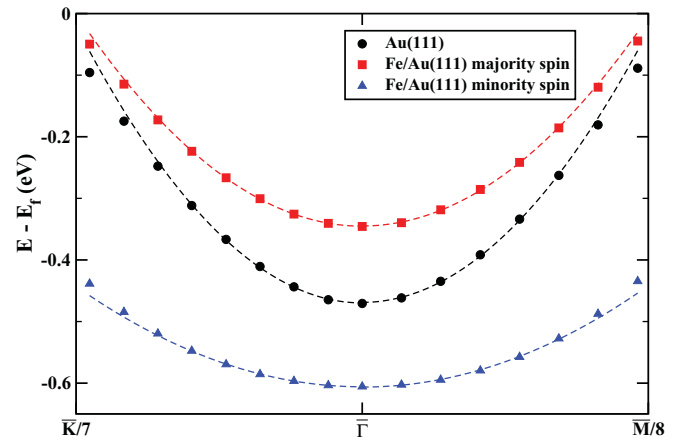


FIG. 4. (Color online) Calculated band dispersion of the Shockley surface state of the clean Au(111) (black circles), Fe/Au(111) majority spin (red squares), and Fe/Au(111) minority spin (blue triangles) along with the fits (dashed line) used to calculate the effective mass for the surface state electrons.

curves and experimental points that we attribute mainly to the inhomogeneity in the shapes of the islands.

In order to get a better understanding of the electronic structure of the Fe islands on the Au(111) surface, we have performed spin-polarized density functional theory calculations. We have used the Quantum-ESPRESSO package¹⁶ with a plane-wave basis set and ultrasoft pseudopotentials.¹⁷ The energy and charge density cutoffs were chosen to be 20 and 160 Ry, respectively, after convergence tests. The local density approximation of the Perdew-Zunger form¹⁸ was used for the exchange-correlation functional. A $(15 \times 15 \times 1)$ Monkhorst-Pack mesh¹⁹ was used for the Brillouin zone integrations along with Methfessel-Paxton smearing technique;²⁰ the smearing width was kept equal to 0.01 Ry. To model the surface, we have used a supercell geometry. The supercell consists of a 39-atomic-layer-thick Au(111) slab with (or without) a pseudomorphic single Fe layer on both sides occupying face-centered sites, separated by 18.7 Å of vacuum.

We first calculated the electronic band structure of clean Au(111) surface and found the Shockley surface state with a band onset and an effective mass close to previous experimental¹⁵ and theoretical results²¹ as reported in Table I. To study the effect of the Fe deposition on the surface state of Au(111), we have calculated the spin-polarized band structure of a Fe monolayer on Au(111). Upon deposition of Fe, we get two different surface states for majority and minority spin electrons. We have calculated various stacking orders and found that Fe on a fcc site is the most stable configuration. The band onset and effective mass of the Shockley state for an Fe layer on fcc sites with a topmost Au layer occupying either fcc or hcp sites are summarized in Table I. The stacking of the top Au layer has only a minor effect on the dispersion of the Shockley surface state. Therefore the effect of substrate stacking at the kink of herringbone reconstruction where the Fe islands are grown can be neglected in our study. The dispersion of the surface states for the most stable configuration (Fe layer and top Au layer on a fcc site) is shown in Fig. 4, in the vicinity of $\bar{\Gamma}$, along the $\bar{\Gamma}\bar{K}$ and $\bar{\Gamma}\bar{M}$ directions.

TABLE I. Band onset E_0 and effective mass of Au(111) and Fe/Au(111) surface states. For the calculations from this work, the stacking of the topmost Au layer is indicated.

Reference	E_0 (meV)	m^*/m_e
Clean Au(111)		
Experiment from Ref. 15	-520	0.26
Calculation from Ref. 21	-510	0.20
Calculation from this work (fcc)	-471	0.20
Calculation from this work (hcp)	-461	0.20
Fe on Au(111)		
Experiment from this work	-420	0.39
Calculation from this work		
Majority spin (fcc)	-346	0.26
Minority spin (fcc)	-606	0.55
Majority spin (hcp)	-356	0.26
Minority spin (hcp)	-614	0.54

However, in the STM experiment we only observe one surface state on the Fe islands. In order to understand this, we calculated the charge density of electrons in the surface state. We found that the majority spin state has an s -like character and extends far into the vacuum, while the minority spin state has a d -like character and is localized on the atoms with a small extension into the vacuum. In the STM experiment, we are sensitive to the LDOS of the sample at the tip location which is several angstroms from the surface, and therefore only the states with a significant charge density at this location can be observed. As a consequence, only the majority spin state that extends into the vacuum could be measured in the experiment. From the calculation, this state should be shifted to a higher energy by about 100 meV as compared with the Shockley surface state of Au(111) while the minority spin state should be shifted to a lower energy than the clean Au(111). Since the band onset deduced from the experiment for Fe/Au(111) is higher than the experimental band onset of Au(111), we can unambiguously identify the measured confined states with the Shockley surface states. Moreover, it is worth noting that both calculation and experiment show that the effective mass of the surface state of Fe/Au(111) is larger than that of a clean Au(111) surface.

B. Spatial analysis

The Shockley states are a model system for a 2D electron gas because they are confined at the surface and act like free electrons in the surface plane. As a consequence, when they are confined in a nanoisland, standing wave patterns develop at the surface of the nanostructure. Figure 5(a) shows the STM image measured at 1 V of an Fe island with an estimated surface area of 10.4 nm². Figures 5(b)–5(e) display the measured dI/dV maps of the first four confined surface states of the island. In addition to the confined states, one can see that the edges of the island appear first dark [Figs. 5(b)–5(d)] and then bright [Fig. 5(e)]. Specific edge features have been observed on Co/Au(111)^{14,22} and Co/Cu(111)¹⁰. In the case of Co/Cu(111) islands, rim states have been clearly identified as spin polarized d states occurring in a narrow range around the Fermi level.¹⁰ In the case of Co/Au(111) edge signatures

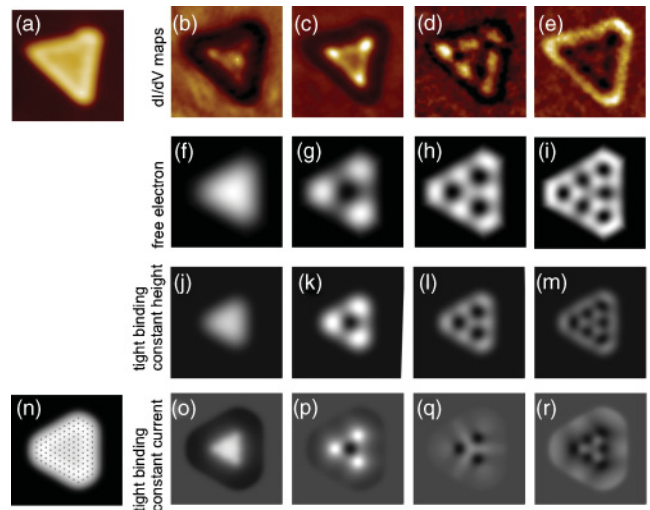


FIG. 5. (Color online) (a) STM topography image of a Fe island on Au(111) (1 V, 500 pA). (b)–(e) Conductance maps of a Fe island on Au(111) at -151 mV, 30 mV, 492 mV, and 955 mV, respectively. (f)–(i) Calculated wave functions at -151 mV, 30 mV, 492 mV, and 1070 mV using a free-electron model in a truncated triangle with a surface of 10.4 nm². (j)–(m) LDOS calculated at the same energies as the experimental images in a horizontal plane using a tight-binding model for an island containing 118 atoms. (n) Simulated topography image at 1 V using a tight-binding model. (o)–(r) LDOS calculated along the simulated topography of the island by the tight-binding model at the same energies as the experimental images.

have been attributed either to spin polarized edge d states²² or to the concentration of excited confined states at the edges of nanoclusters.¹⁴ We will show below that in our case, the dark and bright edge features observed can be explained by the confinement of Shockley surface states. To understand the experimental images, we compared them with calculated wave functions in a truncated triangle. In the following we provide three different descriptions using either a free-electron model or a tight-binding model with image calculation in a plane or along the topography. This provides a direct comparison of the free-electron and tight-binding approximations applied to wave-function calculations in the geometry of our system. The two tight-binding descriptions allow us to reveal the effect of the tip trajectory on the measured conductance maps that has to be taken into account for a proper interpretation of the experimental data.

1. Free-electron model

We have calculated the wave functions of a free particle confined in a truncated triangle with a long to short ratio of 2.73, which corresponds to the shape of the Fe islands investigated. We have adopted the variational method developed by Lijnen *et al.*¹³ and considered a truncated triangle of the same area and at the same energies as in the experimental data [Figs. 5(f)–5(h)]. We have used a Gaussian energy broadening for each electronic state with a standard deviation of 100 meV which mimics the experimental broadening observed in the spectra. Up to the second excited state, the calculated wave functions are very similar to the experimental ones. For the

higher state in Fig. 5(i) the calculation had to be performed at a slightly higher energy (1070 meV) than the experimental data (955 meV) in order to reproduce the features of the experimental dI/dV map. This may be due to the fact that the dispersion of the Shockley state at high energy deviates from a perfect parabola. We will discuss this point in greater detail below.

2. Tight-binding model in a plane

The free-electron model is usually used to describe the Shockley surface states since they correspond to electrons confined at the surface and free to move in the surface plane. However, a tight-binding description can also be instructive for the study of such states,²³ and as we will show it allows a study of the topographical effects on the conductance maps. The dispersion relation for a 2D hexagonal lattice in a first nearest neighbor tight-binding scheme is given by

$$E(k) = \alpha - 2\gamma[\cos(k_x a) + 2\cos(k_x a/2)\cos(k_y a\sqrt{3}/2)],$$

where E is the energy of the surface state, k is the norm of the wave vector of the surface state, α and γ are respectively the Coulomb and overlap integrals, and k_x and k_y are the in-plane components of the wave vector with the x axis pointing along the close-packed direction. For the interatomic distance a we have taken the Au-Au distance (2.88 Å) assuming a pseudomorphic growth of the Fe layer on gold. The effective mass and band onset take the form $m^* = \hbar^2 m_e / 3\gamma a^2$ and $E_0 = \alpha - 6\gamma$, respectively. From the experimental values of m^* and E_0 we can therefore deduce $\alpha = 4.29$ eV and $\gamma = 0.785$ eV. In order to simulate an STM image, we calculated the LDOS around the island in a tight-binding approximation using the following relation:

$$\rho(\vec{r}) = \sum_n \rho_{\text{Fe}}^n(E) |\Phi_n(\vec{r})|^2 + \rho_{\text{Fe}}^0 |\Phi_{\text{Fe}}(\vec{r})|^2 + \rho_{\text{Au}}^0 |\Phi_{\text{Au}}(\vec{r})|^2,$$

where \vec{r} is the location where the LDOS $\rho(\vec{r})$ is calculated. The first term on the right-hand side is the LDOS coming from the eigenstates of the 2D surface states of the Fe island. $\rho_{\text{Fe}}^n(E) = \rho_{\text{Fe}}^{2D} e^{-(E-E_n)/2\sigma^2}$ is the density of states of the n th eigenstate. E_n is the eigenenergy of state n and $\sigma = 100$ meV is the spread in energy of each state evaluated from experimental spectra. $\Phi_n(\vec{r})$ is the n th eigenvector calculated with s -like orbitals for each Fe atom, which gives $\Phi_n(\vec{r}) = \sum_i C_i^n e^{-\|\vec{r}-\vec{r}_i\|/\delta}$. The index i denotes the atoms, C_i^n is the component of the n th eigenstate on the i th atomic orbital, \vec{r}_i is the position of atom i , and δ is the exponential decrease of the s -like atomic orbitals. The second term is an effective term used to represent the electron density coming from Fe states other than the Shockley state with an energy-independent density of states ρ_{Fe}^0 . The corresponding wave function is $\Phi_{\text{Fe}}(\vec{r}) = \sum_i C e^{-\|\vec{r}-\vec{r}_i\|/\delta_{\text{Fe}}}$ where C is a constant, and δ_{Fe} is the exponential decrease of the atomic wave function. The third term corresponds to the Au(111) substrate, and it only depends on the tip to gold surface distance z , where ρ_{Au}^0 is energy independent and $\Phi_{\text{Au}}(\vec{r}) = e^{-z/\delta_{\text{Au}}}$, where δ_{Au} is the exponential decrease for this state. The parameters were obtained from *ab initio* calculations as described below. The value of ρ_{Fe}^{2D} was calculated from the density of states of a 2D electron gas $\rho_{\text{Fe}}^{2D} = m^* S_{\text{at}} / \pi \hbar^2 = 0.078 / (\text{eV}\cdot\text{atom})$

where $S_{\text{at}} = 7.08 \text{ \AA}^2$ is the surface area of the unit cell of the Fe layer. We also obtained $\rho_{\text{Fe}}^0 = 1.98 / (\text{eV}\cdot\text{atom})$ and $\rho_{\text{Au}} = 0.483 / (\text{eV}\cdot\text{atom})$. The decay lengths of the wave functions were found to be $\delta = 1.02 \text{ \AA}$, $\delta_{\text{Fe}} = 0.64 \text{ \AA}$, and $\delta_{\text{Au}} = 0.90 \text{ \AA}$.

Using the expression described above, we calculated the LDOS maps in a horizontal plane (constant height mode) above a truncated triangle island containing 118 atoms with a long to short edge ratio of 2.5 that gives the best agreement with the eigenenergies and shape of the island used in the free-electron model. This ratio is different from that used in the free-electron model due to the atomistic description of the island in the tight-binding approximation that allows only certain values for this ratio. The surface area of this island can be estimated to be $S_{\text{TB}} = n_{\text{at}} \times \Omega = 8.47 \text{ nm}^2$ where $n_{\text{at}} = 118$ is the number of atoms in the island and $\Omega = a^2 \sqrt{3}/2 = 7.18 \text{ \AA}^2$ is the surface area of an unit cell. S_{TB} is smaller than the surface area of the corresponding island in a free-electron model (10.4 nm²). We attribute this to the fact that the Dirichlet condition implies a stronger cutoff of the wave functions at the island edges than the tight-binding model. This means that a larger island has to be used to get a wave function of a given wavelength. The calculated images in Figs. 5(j)–5(m) reproduce well the main features of the experimental conductance maps of Figs. 5(b)–5(e), i.e., a fundamental state followed by excited states similar to the states of a free particle in a box. However, the dark and bright edge effect observed in the experimental dI/dV maps is not reproduced by the calculations. In order to reproduce this effect we have to consider the experimental conditions of the measurements. The conductance maps are not measured in a horizontal plane but are actually measured while the tip follows the profiles of the topographic image. We therefore calculated an image that represents the STM topographic image.

3. Tight-binding model along the tip trajectory

We calculated a map of constant energy integrated LDOS. The resulting image calculated at 1 V is shown in Fig. 5(n) and exhibits edges that appear brighter than the center of the island. This feature results from the addition of the Shockley states at the edges which are integrated in the image. Bright edges are also observed in the experimental images [Fig. 2(a) and Fig. 5(a)] and also could be the result of the addition of Shockley surface states at the edges. We calculated the LDOS at the energies of the experimental dI/dV maps, along the simulated trajectory that reproduces the STM topography. The results reported in Figs. 5(o)–5(r) still display patterns similar to the confined states in the island, but also reproduce an edge effect where the island edge appears dark at low energies and becomes bright when the energy increases. It is consistent with the conductance being measured along the STM topography and not in a plane. This analysis allows us to conclude that the edge effect measured on our system is due to the electron confinement effect. One can, however, notice some discrepancy in the detailed features of calculated and experimental images. The edge appears brighter in the calculation at a lower energy than in the experiment. The edge also appears larger in the calculation at high energy

[Fig. 5(r)] than in the experiment [Fig. 5(e)]. We attribute the discrepancy in these detailed features to the approximation in the shape of the wave functions used in the model, as well as possible difference in the atomic structure of the Fe island in the experiment and in the calculation. However, the trend observed experimentally that edges evolve from dark to bright when increasing the energy is well reproduced by the calculation when the topographic effect is taken into account. Finally, this analysis shows that edge effects observed in the STM images of nanoislands (bright edges in the topography and dark-bright contours in the conductance maps) can be reproduced by a model that only includes the Shockley surface state. Therefore, it can be concluded that such features are not necessarily the signature of specific edge states and can result from confined 2D states in the islands. It is worth noting that the spin polarization of the confined Shockley states should also lead to a spatial modulation of the spin polarization¹¹ of the Fe islands since the spatial variation of the LDOS that we measured comes essentially from the majority spin channel. Turning back to the free-electron calculation at high energy, in Fig. 5(i), as discussed above, we had to use a higher energy than the experimental data. It is interesting to compare this with the tight-binding calculation in Fig. 5(m) that was obtained at the same energy as the experimental data (955 meV). This energy in the tight-binding model corresponds to a wave vector of 0.39 \AA^{-1} . In the free-electron model, this wave vector leads to an energy of 1068 meV, close to what is displayed in Fig. 5(i). This illustrates the fact that the difference between the dispersion curves of the free-electron and the tight-binding models becomes significant at these energies.

IV. CONCLUSION

In conclusion, we have provided experimental data of the electronic structure of Fe nanoislands on Au(111). We have demonstrated the existence of Shockley surface states and determined their effective mass and band onset which is shifted to higher energies as compared with the bare Au(111) substrate. Using a variational approach we have calculated the confined states of a free electron trapped in a truncated island and compared the calculated energies and wave functions with the experimental data. From the calculated wave functions we show that the measured states have the shape of free electronic states confined in the islands. We have shown that these confined states can also be described by a tight-binding approach that also can reproduce the main features of the experimental dI/dV maps. This description of the Fe islands allows us to calculate an STM topography image and to discuss the topography effect on the measured conductance maps, where the edge specific signature can be explained by the confinement of the Shockley states. *Ab initio* calculations demonstrate that the observed Shockley states are spin polarized. These results provide new insight into the electronic and magnetic structure of Fe clusters on Au(111).

ACKNOWLEDGMENTS

We acknowledge financial support from the Indo-French Centre for the Promotion of Advanced Research (CEFIPRA-IFCPAR), the French Ministry of Research, and the Region Ile de France (SESAME).

¹B. Voigtländer, G. Meyer, and N. M. Amer, *Surf. Sci. Lett.* **255**, L529 (1991).

²J. A. Stroschio, D. T. Pierce, R. A. Dragoset, and P. N. First, *J. Vac. Sci. Technol. A* **10**, 1981 (1992).

³W.-C. Lin, H.-Y. Chang, Y.-C. Hu, Y.-Y. Lin, C.-H. Hsu, and C.-C. Kuo, *Nanotechnology* **21**, 015606 (2010).

⁴B. Voigtländer, G. Meyer, and N. M. Amer, *Phys. Rev. B* **44**, 10354 (1991).

⁵D. D. Chambliss, R. J. Wilson, and S. Chiang, *Phys. Rev. Lett.* **66**, 1721 (1991).

⁶C. Boeglin, P. Ohresser, R. Decker, H. Bulou, F. Scheurer, I. Chado, S. S. Dhesi, E. Gaudry, and B. Lazarovits, *Phys. Status Solidi B* **242**, 1775 (2005).

⁷P. Ohresser, N. B. Brookes, S. Padovani, F. Scheurer, and H. Bulou, *Phys. Rev. B* **64**, 104429 (2001).

⁸H. Fujisawa, S. Shiraki, M. Nantoh, and M. Kawai, *Surf. Interface Anal.* **37**, 124 (2005).

⁹L. Niebergall, V. S. Stepanyuk, J. Berakdar, and P. Bruno, *Phys. Rev. Lett.* **96**, 127204 (2006).

¹⁰O. Pietzsch, S. Okatov, A. Kubetzka, M. Bode, S. Heinze, A. Lichtenstein, and R. Wiesendanger, *Phys. Rev. Lett.* **96**, 237203 (2006).

¹¹H. Oka, P. A. Ignatiev, S. Wedekind, G. Rodary, L. Niebergall, V. S. Stepanyuk, D. Sander, and J. Kirschner, *Science* **327**, 843 (2010).

¹²H. Bulou, F. Scheurer, P. Ohresser, A. Barbier, S. Stanesco, and C. Quirós, *Phys. Rev. B* **69**, 155413 (2004).

¹³E. Lijnen, L. F. Chibotaru, and A. Ceulemans, *Phys. Rev. E* **77**, 016702 (2008).

¹⁴K. Schouteden, E. Lijnen, E. Janssens, A. Ceulemans, L. F. Chibotaru, P. Lievens, and C. V. Haesendonck, *New J. Phys.* **10**, 043016 (2008).

¹⁵W. Chen, V. Madhavan, T. Jamneala, and M. F. Crommie, *Phys. Rev. Lett.* **80**, 1469 (1998).

¹⁶P. Giannozzi *et al.*, *J. Phys. Condens. Matter* **21**, 395502 (2009).

¹⁷D. Vanderbilt, *Phys. Rev. B* **41**, 7892 (1990).

¹⁸J. P. Perdew and A. Zunger, *Phys. Rev. B* **23**, 5048 (1981).

¹⁹H. J. Monkhorst and J. D. Pack, *Phys. Rev. B* **13**, 5188 (1976).

²⁰M. Methfessel and A. T. Paxton, *Phys. Rev. B* **40**, 3616 (1989).

²¹J. Henk, M. Hoesch, J. Osterwalder, A. Ernst, and P. Bruno, *J. Phys. Condens. Matter* **16**, 7581 (2004).

²²M. V. Rastei, J. P. Bucher, P. A. Ignatiev, V. S. Stepanyuk, and P. Bruno, *Phys. Rev. B* **75**, 045436 (2007).

²³J. Lagoute, X. Liu, and S. Fölsch, *Phys. Rev. Lett.* **95**, 136801 (2005).